Available online at www.sciencedirect.com
ScienceDirect
Journal of the European Ceramic Society 27 (2007) 4245–4250
www.elsevier.com/locate/jeurceramsoc

Characterisation of two microporous ceramic membranes with different geometrical parameters: Effect of protein adsorption on electrochemical parameters

M.I. Vázquez, R. de Lara, J. Benavente *

Grupo de Caracterización Electrocinética y de Transporte en Membranas e Interfases, Departamento de Física Aplicada I, Facultad de Ciencias, Universidad de Málaga, E-29071 Málaga, Spain

Available online 21 March 2007

Abstract

Two flat ceramic commercial membranes for filtration applications with similar composite structure (a fibrous stain steel network covered by a sublayer of Al_2O_3 particles plus an external layer of ZrO_2) but different "nominal" pore size (25 and 100 nm) are studied. Chemical surface and morphological characterisation was carried out by X-ray photoelectron spectroscopy (XPS) and scanning electronic microscopy (SEM), while transport of NaCl solutions at different concentrations through both membranes was characterized by determining hydraulic and diffusional permeabilities, ion transport numbers and electrical resistance.

Protein adsorption on membrane walls (membrane fouling) was considered by maintaining the membranes in contact with a protein solution for 48 h (2 g/l of bovine seroalbumin or BSA). The effect of protein adsorption on electrochemical parameters was determined by comparing the values obtained with clean and BSA-fouled samples. Results show reduction in diffusional permeability and increase in the electrical resistance (around 20%), but cation transport number hardly depends on membrane fouling.
© 2007 Elsevier Ltd. All rights reserved.

Keyword: Membranes; Porosity; Electrical properties; Electronmicroscopy; Impedance

1. Introduction

Membrane processes for desalination and separation of liquid mixtures are commonly used nowadays.[1] However, filtration of protein or macromolecules as those treated in food and pharmaceutical industries cause important problems associated to membrane fouling, that is, the adsorption/deposition of particles on the membrane surfaces. Cleaning and sterilization procedures used in such systems (high temperature, hard chemicals and radiation) have increased the interest of inorganic membranes due to their better thermal and chemical stability when compared with polymeric membranes,[2] although their higher fragility might reduce their use. Flat ceramic membranes for liquid filtration obtained by particle deposition on a flexible network are already accessible,[3] which are presented as systems combining the most favourable aspects of both inorganic and polymeric membranes, and they are been used in this work.

Chemical surface (XPS analysis) and transport characterizations of two similar flat ceramic membranes (a stain steel network covered by Al_2O_3 and ZrO_2 sublayers), with different nominal pore size (25 and 100 nm) are performed in this work. Membrane transport characterization is carried out with the membranes in "working conditions", that is, in contact with electrolyte solutions and they indicates a weak anionic behaviour for both membranes while differences between "nominal" and estimated geometrical parameters were obtained. Changes in electrochemical characteristic parameters (diffusional permeability, electrical resistance and ion transport numbers) as a result of protein (BSA) adsorption on the membrane surfaces was also considered by comparing results obtained with clean and BSA-fouled samples. A reduction in the porosity of both fouled membranes was obtained from diffusional permeability and electrical resistance results, but ions transport numbers (relative fluxes) hardly vary for the studied samples.

* Corresponding author. Tel.: +34 952131929; fax: +34 952132000.
E-mail address: j_benavente@uma.es (J. Benavente).

0955-2219/$ – see front matter © 2007 Elsevier Ltd. All rights reserved.
doi:10.1016/j.jeurceramsoc.2007.02.141

2. Experimental

2.1. Membranes and solutions

Two microporous ceramic membranes CREAFILTER Z25S and Z100S from Degussa (Germany) with nominal thickness between 80 and 100 μm, and nominal pore size of 25 (sample Z25S) and 100 nm (sample Z100S) were studied.[3] According to the suppliers, the membranes present a composite structure formed by a fibrous stain steel network covered by a sublayer of Al_2O_3 particles plus an external layer of ZrO_2, and this complex structure made necessary the estimation of effective geometrical parameters; that is, the surface area and thickness corresponding to the ceramic porous material crossed by the flow (without including the impenetrable stain steel support), which clearly differ from the values determined by usual methods (f.i., a micrometer), other information related to membrane geometry can be found in the literature.[3,4]

Protein-fouled membranes were achieved by maintaining one of the membrane surfaces in contact with a solution containing 2 g/l of bovine serum albumin (BSA) for 48 h. The fouled samples will hereafter name Z25S + 48BSA and Z100S + 48BSA.

2.2. Chemical surface and morphological characterization

Surface chemical characterisation was carried out by XPS using a Physical Electronics PHI 5700 spectrometer with a non-monochromatic Mg Kα radiation (300 W, 15 kV, 1253.6 eV) as excitation source. High-resolution spectra were recorded at 45° take-off-angle by a concentric hemispherical analyser operating in the constant pass energy mode at 29.35 eV, using a 720 μm diameter analysis area. Other equipment characteristics and experimental procedure are indicated in Refs. 5,6.

Membrane scanning electron micrographs were recorded by using a JEOL JSM-6400 scanning electron microscope (SEM). Samples were coated with a thin layer of gold before microscopy examination.

2.3. Determination of transport characteristic membrane parameters

Hydrodynamic permeability was determined from the volume flow–pressure measurements by using a cross-flow cell (Minitan II, Millipore), with an exposed membrane area of 59.2 cm^2 and re-circulation in feed and permeate solutions.[7] Water and NaCl solutions were used and the applied pressure ranged between 75 and 400 kPa.

Salt diffusion, membrane potential and impedance spectroscopy measurements were carried out in a "dead-end" test cell similar to that described elsewhere.[8] The membrane was tightly clamped between two glass half-cells, which have magnetic stirrers at the bottom to minimise concentration–polarisation at the membrane surfaces (stirring rate of 525 rpm).

- In salt diffusion measurements the membrane was initially separating a concentrated solution, c_1, from a diluted one (initially, $c_2 = 0$). Changes in solution c_2 were recorded versus time by means of a conductivity cell connected to a digital conductivity meter (Radiometer CDM 83). Diffusion measurements with membranes Z25S and Z100S were performed at five different c_1 constant concentrations ($0.005 \leq c$ (M) ≤ 0.1 M), while for both fouled membranes only the higher concentrations were studied ($c_1 = 0.05$ and 0.1 M NaCl).
- The electromotive force (ΔE) between both sides of a membrane caused by a concentration gradient was measured by two reversible Ag/AgCl electrodes connected to a digital voltmeter (Yokohama 7552). Measurements for clean and fouled samples were carried out by keeping the concentration c_1 at one side of the membrane constant ($c_1 = 0.01$ M) and gradually changing the concentration of the solution at the other side, c_2, from 10^{-3} to 0.1 M.
- Impedance spectroscopy (IS) measurements were performed by using an Impedance Analyzer (Solartron 1260) controlled by a computer. The data were corrected by software and the influence of connecting cables and other parasite capacitances. The measurements were carried out using 100 frequencies in the range 1 to 10^7 Hz at a maximum voltage of 0.01 V, the solutions at both sides of the membrane having the same concentration (0.001, 0.002, 0.005 and 0.01 M for Z25S and Z100S membranes, and 0.001 M for both fouled samples).

All these measurements were performed at room temperature (25.0 ± 0.5) °C and standard pH (5.9 ± 0.3).

3. Results and discussion

Membrane surface chemical characterization was carried out from XPS analysis. Relative atomic concentrations (AC%) of the elements present in the surface of Z25S and Z100S are indicated in Table 1 (average of three measurements). There are two significant points in the values shown in Table 1: (i) the high atomic concentration percentage of carbon, which is partially associated to membrane manufacture compounds, but environmental contamination must also be considered[9]; (ii) the low atomic concentration percentage of zirconium on the surface of Z100S membrane. This latter result seems to indicate that Z100S sample could practically be considered as an alumina membrane; then, possible differences in some membrane parameters might exist, which could be related to the different membrane materials.

SEM micrographs of membrane Z25S is shown in Fig. 1. This picture permits us to estimate the effective "ceramic membrane" thickness, $\Delta x_m(ef) = (60 \pm 5)$ μm and area, $S_m(ef) \cong 40\% S_m$, related to the transport of solution or ion fluxes, where S_m rep-

Table 1
Atomic concentration percentages of different elements on the surface of ceramic Z25S and Z100S membranes

Membrane	⟨C 1s⟩ (%)	⟨O1s⟩ (%)	⟨Zr 3d⟩ (%)	⟨Al 2p⟩ (%)
Z25S	17.7 ± 2.3	53.7 ± 1.1	20.4 ± 1.4	8.2 ± 1.5
Z100S	16.0 ± 1.5	51.5 ± 1.0	2.2 ± 0.1	30.1 ± 0.8

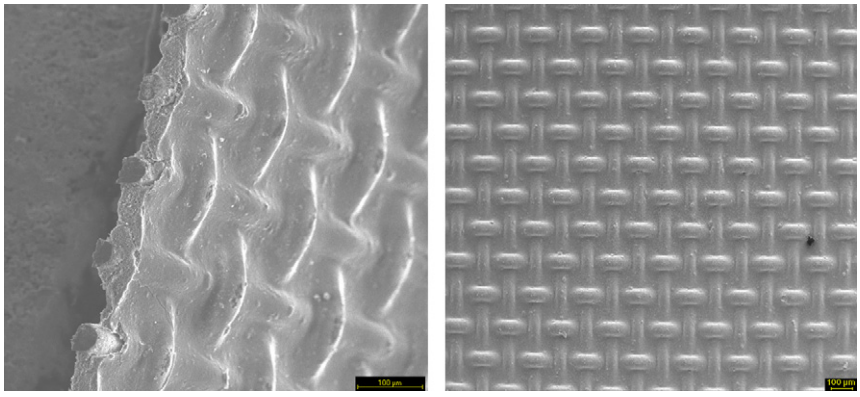

Fig. 1. Cross-section and surface SEM micrographs for membrane Z25S (black mark = 100 μm).

resents the cell hole where membrane was placed (it depends on the cell system used); surface and thickness effective values were determined by subtracting the contribution of the stain steel fibres as was previously indicated, and practically the same values for Z25S and Z100S were obtained.

The flux of solute through a membrane, J_s, and the concentration difference causing the flux, Δc, are related by the diffusional or salt permeability, $J_s = P_s \Delta c$, and it can be written[1]:

$$J_s = \left[\frac{dn}{dt}\frac{1}{S_m}\right] = \frac{V_0}{S_m}\frac{dc_2}{dt} = P_s \Delta c = P_s(c_1 - c_2(t)) \quad (1)$$

where S_m and V_0 are the membrane area expose to flux and the volume of the solution at the side of concentration c_2. For a quasi-steady state (J_s = cte) and considering solution conductivity instead of concentration, the following expression can be obtained:

$$\frac{d\sigma_2}{c_1 - \sigma_2(t)} = \frac{S_m}{V_0}\left(\frac{d\sigma}{dc}\right)_e P_s\, dt \quad (2)$$

where $(d\sigma/dc)_e$ is an electrolyte characteristic parameter at a given temperature. Eq. (2) allows the determination of P_s by measuring solution conductivity σ_2 as a function of time. Fig. 2 shows the σ_2–t relationships for Z25S and Z100S membranes at a given concentration (c_1 = 0.05 M NaCl); from the slopes of these straight lines, diffusional permeability across the membrane was obtained by Eq. (2), and their average values for the whole interval of concentration are indicated in Table 2. Results show that diffusional permeability for Z25S sample is lower (85% approximately) that for membrane Z100S, which could be due to differences in geometrical parameters or solute/membrane interactions. For a porous membrane, P_s is given by[1]: $P_s = (D_s \Theta/\Delta x_m)$, where D_s is the salt diffusion coefficient in the membrane, Θ and Δx_m are the membrane porosity and thickness, respectively. From average diffusional permeability value for membrane Z100S, assuming $D_s = D_s^\circ$ (solution diffusion coefficient) due to its high pore size, a porosity around 20% was obtained; however, for Z25S membrane differences between D_s and D_s° could also exist due to its (nominal) low pore radii.

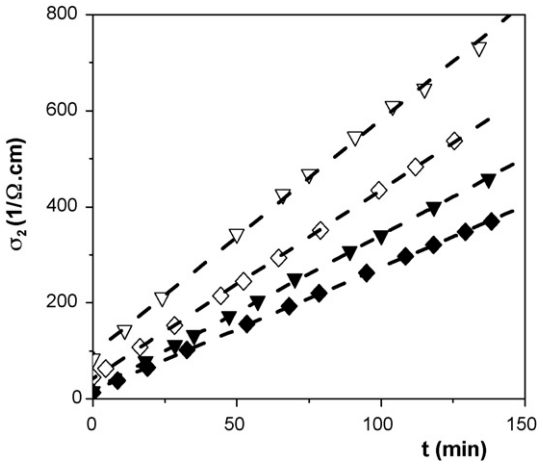

Fig. 2. Solution conductivity, σ_2, vs. time for membranes: Z25S (◊); Z25S + 48BSA (♦); Z100S (▽); Z100S + 48BSA (▼). c_1 = 0.05 M NaCl.

For comparison, Fig. 2 also shows solution conductivity–time dependence for fouled membranes, Z25S + 48BSA and Z100S + 48BSA samples, at the same constant concentration. Diffusional permeability for both fouled samples are indicated in Table 2, as can be observed lower permeability values for fouled samples were obtained (a reduction around 25%), which could be attributed to a decrease in the porosity of the fouled membrane as a result of protein adsorption.

Other characteristic membrane parameter connecting membrane transport and geometrical parameters is the hydraulic or hydrodynamic permeability, $L_p = (J_v/\Delta P)_{\Delta c=0}$, which is determined by measuring the volume flow through the membrane, J_v, under a pressure difference, ΔP. Fig. 3 shows hydraulic permeability–concentration dependence for both membranes and as can be observed lower values were also obtained for Z25S sample $(L_p^{Z25S}/L_p^{Z100S} = 0.8)_{water}$, even when distilled water was used, in agreement with diffusional permeability values.

Table 2
Average membrane cation transport number, $\langle t_+ \rangle$, and diffusional permeability, $\langle P_s \rangle$, for clean and protein-fouled membranes

Membrane	$\langle t_+ \rangle$	$\langle P_s \rangle$ ($\times 10^{-6}$ m/s)
Z25S	0.340 ± 0.003	4.63 ± 0.12
Z25S + 48BSA	0.375 ± 0.006	3.68 ± 0.05
Z100S	0.341 ± 0.004	5.48 ± 0.18
Z100S + 48BSA	0.350 ± 0.005	3.80 ± 0.17

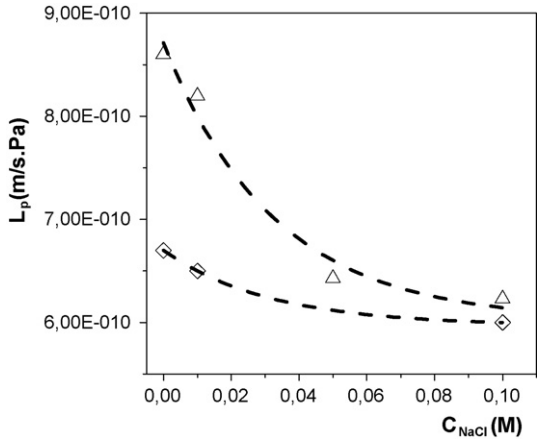

Fig. 3. Membrane hydrodynamic permeability vs. salt concentration: (◊) Z25S; (▽) Z100S.

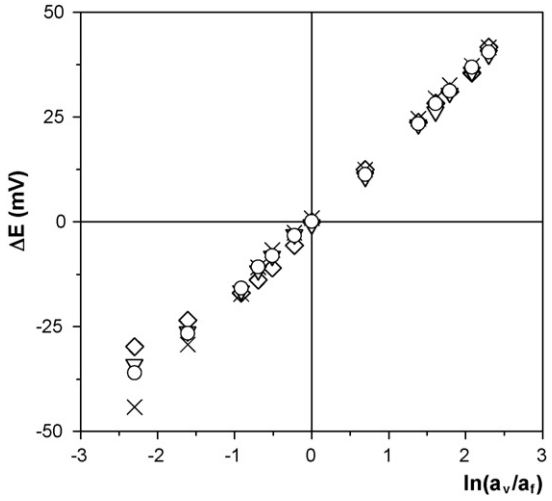

Fig. 4. Measured potential difference, ΔE, versus solution activity ratio for the different membranes studied: (◊) Z25S; (▽) Z100S; (×) Z25S + 48BSA; (◯) Z100S + 48BSA.

For an ideal porous membrane L_p can be related with geometrical parameters assuming the validity of the Poiseulle–Haagen equation, then[1]: $L_p = (\Theta r_p^2)/(8\Delta x_m \eta)$, where r_p is the equivalent pore radius and η is the solution viscosity. Taking into account hydrodynamic permeability and the porosity previously determined from diffusion results for Z100S sample, a pore radii of 45 nm is obtained; this value is in very good agreement with its nominal value (50 nm), and it can also serve as a probe of the reliability of the other two parameters, thickness and porosity, assumed for Z100S sample. Considering these values also valid for membrane Z25S, a pore radii of 40 nm was obtained, which is three times higher than the nominal value indicated by the suppliers (if 45% porosity is considered $r_p^{Z25S} \approx 27$ nm).

When transport of electrolyte solutions or charged macromolecules across a membrane is considered, determination of its electrical parameters is of great interest. The electrical potential difference measured at both sides of a membrane separating two solutions of the same electrolyte but different concentrations is ΔE (which also includes the electrode contribution), and its expression for a 1:1 electrolyte is[10]:

$$\Delta E = -\left(\frac{2RT}{F}\right) t_+ \ln\left(\frac{a_1}{a_2}\right) \quad (3)$$

where a_i is the solution activity, R and F are the gas and Faraday constants and T is the thermodynamic temperature of the system. The ion transport number, $t_i = I_i/I_T$, represents the amount of current transported for one ion with respect to the total current crossing the membrane, then $t_+ + t_- = 1$. Fig. 4 shows the linear dependence between ΔE and $\ln(a_1/a_2)$, which allows the determination of average cation transport number in the studied membranes (clean and fouled samples) $\langle t_+ \rangle$, from the slopes of the straight lines in Fig. 4 and they are indicated in Table 2. Cation transport number in the membranes are practically independent of both pore radii and fouling since it correspond to a relative flux,[11] although the presence of BSA seems slightly increase the cation flux.

Fig. 5a shows the impedance plot (Nyquist plot, $-Z_{img}$ versus Z_{real}) for membranes Z25S, Z100S and both fouled samples. The analysis of impedance is usually carried out by the complex plane Z^*, where a single parallel resistance–capacitor (R–C) circuit gives rise to a semi-circle as that shown in Fig. 5a, which has intercepts on the Z_{real} axis at R_∞ ($\omega \to \infty$) and R_0 ($\omega \to 0$), being $(R_0 - R_\infty)$ the resistance of the system; the maximum of the semi-circle equals $0.5(R_0 - R_\infty)$ and it occurs

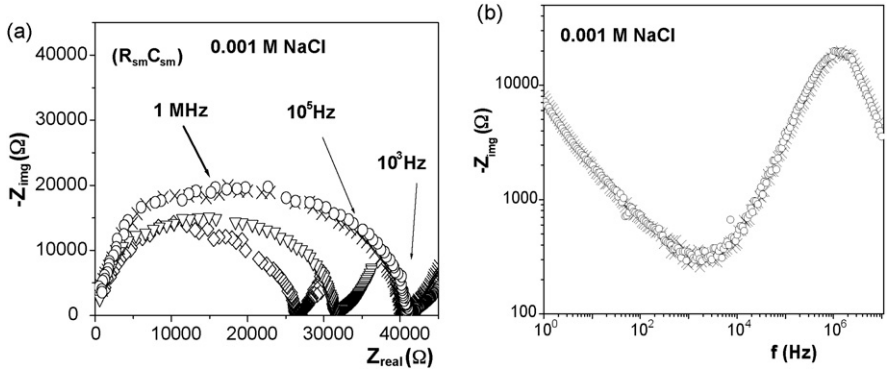

Fig. 5. Impedance plots. (a) Nyquist plot for the studied membranes: (◊) Z25S; (▽) Z100S; (×) Z25S + 48BSA; (◯) Z100S + 48BSA. (b) Bode plot for both fouled membranes: (×) Z25S + 48BSA; (◯) Z100S + 48BSA.

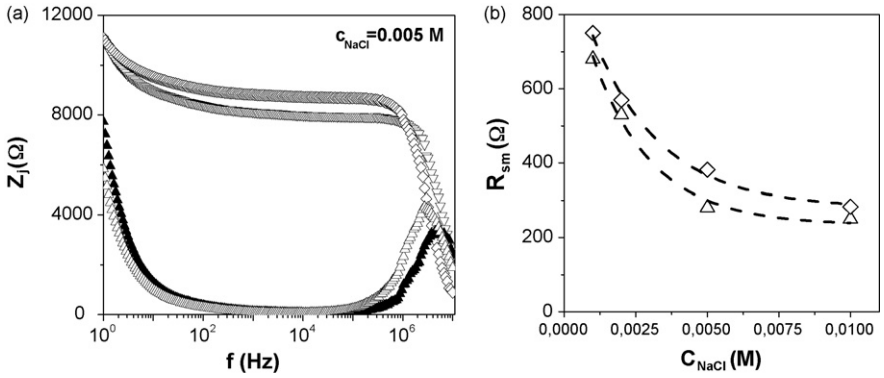

Fig. 6. (a) Comparison of Bode plots for both clean membranes. Z25S sample: (◊) real part; (△) imaginary part; Z100S sample: (▽) real part; (▲) imaginary part. (b) Variation of membrane system electrical resistance, R_{sm}, with salt concentration: (◊) Z25S sample; (▽) Z100S sample.

at an angular frequency (ω) such that $\omega RC = 1$, being $\tau = RC$ the relaxation time.[12] Bode plots ($-Z_{img}$ versus f, or Z_{real} versus f) is another impedance plot, and it allows the estimation of the frequency range associated to a given relaxation process as is shown in Figs. 5b and 6a. A unique relaxation process was obtained for all the "membrane systems" studied, that is, the membrane and the electrolyte solution placed between the electrodes and the membrane surfaces, as was reported in the literature for highly porous membranes.[13,14] Differences in Z_{img} values for Z25S and Z100S membranes indicate different ion adsorption on the membrane, which could be associated to differences in surface membrane materials (ZrO_2 for sample Z25S and Al_2O_3 for Z100S) in agreement with XPS results.

The fitting of the experimental points as those indicated in Fig. 5a by means of a non-linear program[15] allows the determination of the membrane system electrical resistance, R_{sm}. Variation of R_{sm} with salt concentration for Z25S and Z100S membranes is shown in Fig. 6b, where the differences obtained are associated to differences in the membrane geometrical parameters; the following value for the average resistance ratio was obtained, $\langle R_{sm}^{Z100S}/R_{sm}^{Z25S}\rangle = (0.86 \pm 0.08)$, which is in concordance with hydrodynamic results.

Differences between clean and fouled membranes are also observed when the impedance plots are compared (see Fig. 5a). An increase in the electrical resistance of both fouled samples was obtained, in agreement with the lower porosity assumed from diffusional permeability results. However, impedance plots for fouled membranes hardly differ one from each other: $R_{sm}^{Z25S+48BSA}/R_{sm}^{Z100S+48BSA} = 0.92$, and similar Z_{img} values were obtained as can be observed in Fig. 5b; this last point seems to indicate that BSA complete covers the membrane surfaces, since no differences in adsorption attributed to different materials are obtained with fouled samples.

4. Conclusions

Two ceramic composite membranes for liquid filtration application were characterized by determining surface chemical composition and transport parameters under common "membrane working conditions". This latter characterization allows the estimation of geometrical parameters, which were compared with "nominal" ones.

Protein adsorption on the membrane surfaces (membrane fouling) can modify some of these parameters causing a reduction of diffusional permeability and an increase of electrical resistance, both parameters dependent on membrane porosity, and their modifications indicate porosity reduction as a result of membrane fouling. Capacitive effects obtained from IS measurements are related to charge adsorption and differences among the studied samples are attributed to differences in the membrane surface material in agreement to XPS results.

References

1. Mulder, M., *Basic Principles of Membrane Technology*. Kluwer Academic Publishers, Dordrecht, The Netherlands, 1992.
2. Bhave, R. R., *Inorganic Membranes: Synthesis, Characteristics and Applications*. Van Nostrand Reinhold, New York, 1991.
3. Augustin, S., Hennige, V., Hörpel, G. and Hying, Ch., Ceramic but flexible: new ceramic membrane foils for fuel cells and batteries. *Desalination*, 2002, **146**, 23–28.
4. de Lara, R., Galán, P., Muñoz, A. and Benavente, J., Caracterización electrocinética de membranas porosas: efecto de la radiación. In *Proceedings of the XII Iberic Electrochemical Meeting*, 2006, p. 6.
5. Moulder, J. F., Stickle, W. F., Sobol, P. E. and Bomben, K. D., In *Handbook of X-ray Spectroscopy*, ed. J. Chastain. Perkin-Elmer Corp., 1992.
6. Cañas, A., Ariza, M. J. and Benavente, J., Characterization of active and porous sublayers of a composite reverse osmosis membrane by impedance spectroscopy, streaming and membrane potentials, salt diffusion and X-ray photoelectron spectroscopy. *J. Membr. Sci.*, 2001, **183**, 135–146.
7. Cañas, A., Vázquez, M. I. and Benavente, J., Effect of polarisation layers on salt permeability across membranes with different structures. *Desalination*, 2002, **146**, 163–167.
8. Benavente, J., Muñoz, A. and Heredia, A., Electrokineic characterization of isolated pepper cuticles in protonic forms. *Solid State Ionics*, 1997, **97**, 89–95.
9. Keurenjes, J. T. F., Harbrecht, J. G., Brinkman, D., Hanemaaijer, J. H., Cohen, M. A. and van't Riet, H., Hydrophobicity measurements of microfiltration and ultrafiltration membranes. *J. Membr. Sci.*, 1989, **47**, 199–205.
10. López, M. L., Compañ, V., Garrido, J., Riande, E. and Acosta, J. L., Proton transport in membranes prepared from sulfonated polystyrene–poly(vinylfluoride) blends. *J. Electrochem. Soc.*, 2002, **148**, 372–376.
11. Benavente, J., Vázquez, M. I. and de Lara, R., Modification of active and porous sublayers of aged polyamide/polysulfone composite membranes due

to HNO_3 treatment: effect of treatment time. *J. Colloid Interf. Sci.*, 2006, **297**, 226–234.
12. Macdonald, J. R., *Impedance Spectroscopy*. Wiley, New York, 1987.
13. Asaka, A., Dielectric properties of cellulose acetate reverse osmosis membranes. *J. Membr. Sci.*, 1990, **50**, 71–80.
14. Benavente, J., Ramos-Barrado, J. R., Bruque, S. and Matinez, M., Determination of some electrical parameters for $UO_2(O_3PC_6H_5)$ films deposited on a porous support. *J. Chem. Soc. Faraday Trans.*, 1994, **90**, 3103.
15. Boukamp, B. A., A package for impedance/admittance data analysis. *Solid State Ionics*, 1986, **18&19**, 136.